



UvA-DARE (Digital Academic Repository)

Epigenetic control of hippocampal stem cells: modulation by hyperactivation, glucocorticoids and aging

Schouten, M.

Publication date

2015

Document Version

Final published version

[Link to publication](#)

Citation for published version (APA):

Schouten, M. (2015). *Epigenetic control of hippocampal stem cells: modulation by hyperactivation, glucocorticoids and aging*. [Thesis, fully internal, Universiteit van Amsterdam].

General rights

It is not permitted to download or to forward/distribute the text or part of it without the consent of the author(s) and/or copyright holder(s), other than for strictly personal, individual use, unless the work is under an open content license (like Creative Commons).

Disclaimer/Complaints regulations

If you believe that digital publication of certain material infringes any of your rights or (privacy) interests, please let the Library know, stating your reasons. In case of a legitimate complaint, the Library will make the material inaccessible and/or remove it from the website. Please Ask the Library: <https://uba.uva.nl/en/contact>, or a letter to: Library of the University of Amsterdam, Secretariat, P.O. Box 19185, 1000 GD Amsterdam, The Netherlands. You will be contacted as soon as possible.

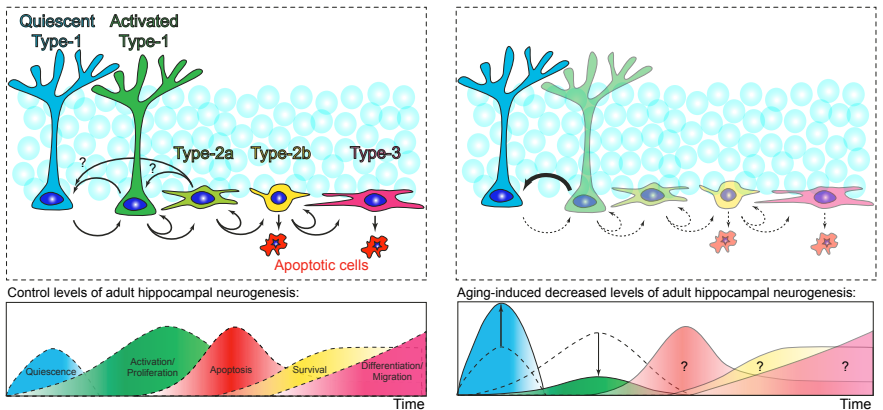
6

Age-related decline of hippocampal neural precursor cell populations is associated with expression of the glucocorticoid receptor

Marijn Schouten, Pascal Bielefeld, Paul J. Lucassen and Carlos P. Fitzsimons

In preparation

Graphical abstract



Schematic depiction of the initial stages of the neurogenic cascade in control animals (left) or aged animals (right). Phenotypical alterations are: increased quiescence and decreased proliferation. In this chapter we discuss that glucocorticoid receptor expression in neural precursor cells is associated with different age-related decay kinetics.

Abstract

Aging is associated with alterations in neuro-endocrine functions, including a dysregulation of the hypothalamo-pituitary-adrenal (HPA) axis and glucocorticoid levels. This dysregulation coincides with cognitive impairments and an overall decrease in hippocampal neural precursor cell (NPC) proliferation. NPC sensitivity to glucocorticoids has been found to change with age, with a significant increase in glucocorticoid receptor (GR) expression present in the quiescent and activated neural stem/progenitor cell populations, known as type-1 and type-2 cells. So far, a more detailed characterization of the GR in NPC populations and their dynamics with age is lacking.

Here, we used Nestin-GFP mice to characterize age-related changes in specific NPC populations, and investigated their relationship with GR (co-)expression in hippocampi of 3 age groups: young, young adult and middle-aged mice. We used linear and non-linear models to characterize the relative decay of the type-1 and type-2 NPC subsets. Our results demonstrate that the presence or absence of GR expression identifies different NPC populations. We found that type-1 and type-2 NPCs expressing the GR followed linear age-related decay kinetics, whereas type-1 and type-2 NPCs lacking GR followed non-linear decay kinetics. Interestingly, although NPCs lacking GR expression were readily identified at young ages, NPC populations lacking GR expression were rare in young adult and middle-aged mice, suggesting either an age-dependent GR upregulation in NPCs or alternatively, a higher age dependent decline of this subpopulation. Although all NPC populations decreased in number with age, populations expressing GR typically displayed slower decay kinetics, suggesting a role for the GR in NPC population maintenance during aging.

Introduction

Following exposure to stress, the HPA axis is activated, releasing several hormones that mediate the stress response. Among these, glucocorticoids hormones (CORT) are powerful mediators released from the adrenal cortex following circadian as well as ultradian rhythms¹. These pulsatile release patterns are affected by stressors such as sleep deprivation, chronic psychological stress², and age³⁻⁵. In particular, a reduction in the amplitude of the circadian CORT rhythm has been associated with aging, largely resulting from elevations in evening CORT levels⁶ and decreases in diurnal CORT⁷. This altered endocrine profile correlates with a decline in hippocampus-related cognition⁸. The hippocampus contains NPCs that continue to form new neurons throughout adulthood. This process of 'adult hippocampal neurogenesis' (AHN) has been implicated in hippocampus-related cognition, including spatial memory⁹, HPA axis regulation¹⁰ and shows a marked age-associated decline, particularly in the proliferation and differentiation capacity of the hippocampal NPCs^{11,12}.

AHN is a multistep process in which radial glia/astrocyte-like cells act as neural stem cells (NSC), that generate transit-amplifying neural progenitors^{13,14}. These, in turn, proliferate and differentiate into new neurons that eventually integrate into the pre-existing hippocampal network¹⁵. Radial glia-like astrocytes, or type-1 cells are largely quiescent, whereas type 2 cells, called transit-amplifying progenitor cells, undergo proliferation in the adult hippocampus^{16,17}. Type-1 can be distinguished from type-2 NPCs based on their morphology and the expression of specific markers such as the glial fibrillary acidic protein (GFAP), or, when using Nestin-GFP transgenic mice, on the co-expression of GFP driven by the Nestin promoter^{16,18}.

Previous results from our lab had indicated that GR expression in NPCs is crucial for AHN regulation under non-stress conditions in young mice, suggesting that the GR is a crucial mediator of CORT effects on NPCs¹⁹. However, little is known about the effect of age on GR expression in NPCs. Previous studies identified GR in early stages of AHN^{20,21}, where significant differences were found in GR expression in the type-1 and

-2 NPCs between young (7 weeks-old) and old (20 months-old) mice²¹. Others found an age-related decline in murine hippocampal NPC with a marked deflection point around 6 months of age²².

Therefore, we here analyzed GR co-expression in type-1 and type-2 NPCs in three age groups: young adult (3 months), mature adult (6 month) and middle-aged (10 months) C57BL/6j mice as defined by Flurkey *et al.*²³. We used a Nestin-GFP transgenic strain in which GFP expression selectively labels NPCs¹⁸. We sought to address the rate of NPC population decay and used linear and non-linear model equations to characterize the type-1 and type-2 NPC population dynamics. Our results confirm the presence of GR+ and GR- type-1 and type-2 NPC populations in young adult animals as previously described. However, we observed a strong predominance of the GR+ NPC phenotype in mature adult and middle-aged mice. Interestingly, GR- and GR+ type-1 and type-2 NPC populations followed non-linear and linear decay curves, respectively, with age.

Materials and methods

Animals, immunohistochemistry and confocal microscopy.

Male 1, 3, 6 and 10 month old Nestin-GFP transgenic mice¹⁸ (n=3 per group) were used for immunocytochemistry. Mice were single housed under standard laboratory cage conditions and kept under 12hour light/dark cycles with ad libitum access to food and water. At the indicated ages, animals were transcardially perfused with 4% paraformaldehyde in PBS and brains were extracted, sectioned in 8 series of at 40µm and immunostained as described before¹⁹, using the following antibodies: polyclonal chicken anti-GFP (Abcam. 1:500), monoclonal mouse anti-GFAP (Chemicon. 1:1000) and polyclonal rabbit anti-GR (H300 Santa Cruz. 1:100) in combination with goat anti-chicken Alexa488 (Invitrogen. 1:500), goat anti-mouse Alexa647 (Invitrogen. 1:500) and goat anti-rabbit Alexa568 (Invitrogen. 1:500), respectively. Sections were counterstained for DNA using Hoechst (Invitrogen. 1:20000) to detect cell nuclei. Confocal microscopy was performed as described before using a Zeiss LSM510 laser scanning microscope¹⁹. Quantifications of hippocampal NPC populations were

performed only on the adult age groups (3, 6 and 10 months) as described before²⁴ and were either expressed in absolute numbers per hippocampus or in relative percentages of total NPC subpopulation.

Generation of best-fit curves and statistical analysis.

Second order polynomial best-fit curves ($y(x) = ax^2 + bx + c$) including their 95% confidence intervals were based on the absolute numbers of GR+ and GR- type-1 and type-2 adult NPCs per hippocampus derived from 3, 6 and 10 month old Nestin-GFP transgenic mice, using Graphpad Prism 5.0 software. Second order polynomial best fit curves were statistically compared to a first order polynomial curve fitting ($y(x) = ax + b$) using an extra-sum-of-squares F-test and they were considered significantly different if the extra-sum-of-squares F-test reached a $p < 0.05$. Subsequently, curve parameters such as increment and slope from GR+ and GR- type-1 and type-2 NPC were compared using an extra-sum-of-squares F-test. The calculated parameters were considered significantly different when the extra-sum-of-squares F-test reached a $p < 0.05$. All other comparisons were statistically tested using one-way analysis of variance (ANOVA) test with a Tukey's post-hoc test. Graphpad Prism 5 software was used for the generation of best-fit curves and statistical analysis.

Results

Nestin-GFP, GFAP and GR immunoreactivity was readily detectible in the subgranular zone (SGZ) of the dentate gyrus of animals from 1 month up to 10 months of age (Figure 1A-D). Based on the expression of these 3 markers, NPC were classified in different subtypes, using a previously described system of developmental milestones^{16,17,21}. Based on their GFAP (co-)expression, type-2 NPCs can be further separated into type-2a (Nestin-GFP+/GFAP+) and type-2b (Nestin-GFP+/GFAP-)NPCs¹⁷. In the brains of adult animals (i.e. 3 months or older), the type-1, -2a and -2b NPCs could be clearly identified (Figure 2A-F). In contrast to previous observations²⁵, we observed a significant age-related decrease in the type-1 cells numbers between young adult, mature adult and middle-aged mice ($p < 0.01$) (Figure 1E). The same applied to the type-2a cell numbers (Figure 1E). Importantly, a more marked age-related decrease was found in type-2b cell numbers

(Figure 1E), that were the largest NPC population in young adult animals and became the smallest population in mature adult and middle-aged mice (Figure 1E).

As the GR is an important regulator of NPCs^{19,26}, differential GR expression in NPC subpopulations²¹ could provide a possible explanation for the differential sensitivity to GCs. To test this, we characterized GR expression in type-1 and type-2 cells of the three adult age groups included in this study and observed a significant age-related decay in the relative abundances of GR+ type-1, type-2a and type-2b cells (Figure 2G). We observed that $86.8 \pm 3.7\%$ of type-1 cells and $71.6 \pm 9.3\%$ of type-2a cells were GR+ in Nestin-GFP transgenic mice at 3 months of age (Figure 2G). Notably, we found that $31.3 \pm 8.5\%$ of type-2b cells were GR+ (Figure 2G).

We next characterized age-related patterns in the expression of GR+ and GR- type-1 and type-2 cell numbers using linear and non-linear models of cell-population dynamics. We tested whether GR+ and GR- type-1 and type-2 cell numbers fitted better to a first order polynomial equation (linear dynamics model), or to a second order polynomial equation (non-linear dynamics model) (Figure 3A-F and Tables 1-3). Interestingly, the cell population decay of GR+ type-1 (Figure 3A; Table 1), type-2a (Figure 3C; Table 2) and type-2b (Figure 3E; Table 3) cells fitted best to a linear dynamics model, while the cell population decay of type-1/GR- (Figure 3B; Table 1) and type-2b/GR- (Figure 3F; Table 3) cells showed fitted best to a non-linear dynamics model. GR-Type-2a cells, however, fitted best to a linear dynamics model (Figure 3D; Table 2).

Next, we directly assessed whether GR expression significantly affected age-related population dynamics in type-1, type-2a and type-2b NPC populations (Figure 3G-I and Table 4). To this aim, for type-1 and type-2b cells we compared specific non-linear dynamics model curve parameters between GR+ and GR- subsets (Figure 3G and 3I, Table 4) and for type-2a we compared specific linear dynamics model curve parameters between GR+ and GR- subsets (Figure 3H, Table 4). The parameters used for comparison included increment (initial number of cells) and slope (decay kinetics of NPC). The curve fit corresponding to

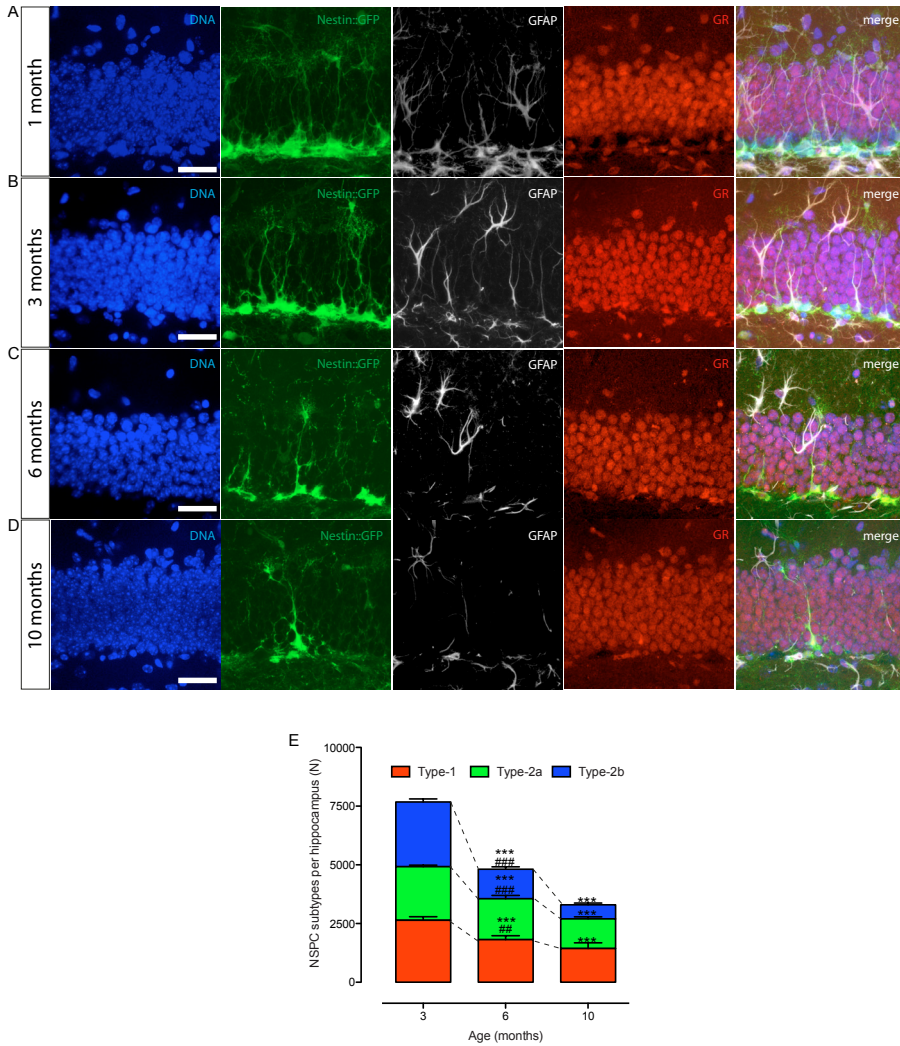


Figure 1 - Nestin-GFP expressing NPC subsets decrease with age. (A) Representative confocal micrograph showing Nestin-GFP (green), GFAP (white) and GR (red) immunoreactivity in the DG of a young mouse of 1 month of age. Nuclei are visualized by a Hoechst staining (blue). (B) Representative confocal micrograph showing Nestin-GFP (green), GFAP (white) and GR (red) immunoreactivity in the DG of an adult mouse of 3 months of age. Nuclei are visualized by a Hoechst staining (blue). (C) Representative confocal micrograph showing Nestin-GFP (green), GFAP (white) and GR (red) immunoreactivity in the DG of an adult mouse of 6 months of age. Nuclei are visualized by a Hoechst staining (blue). (D) Representative confocal micrograph showing Nestin-GFP (green), GFAP (white) and GR (red) immunoreactivity in the DG of an adult mouse of 10 months of age. Nuclei are visualized by a Hoechst staining (blue). (E) Bar graph depicting the numbers of type-1 (red), type-2a (green) and type-2b (blue) NPC per hippocampus at 3, 6 and 10 months of age. Data are expressed as mean±SEM of three animals and statistically tested for differences (***) $p < 0.001$ compared to 3 months or for differences (##) $p < 0.01$, (###) $p < 0.001$ compared to 10 months using one-way analysis of variance. Scale bars represent 50 μm (A-D).

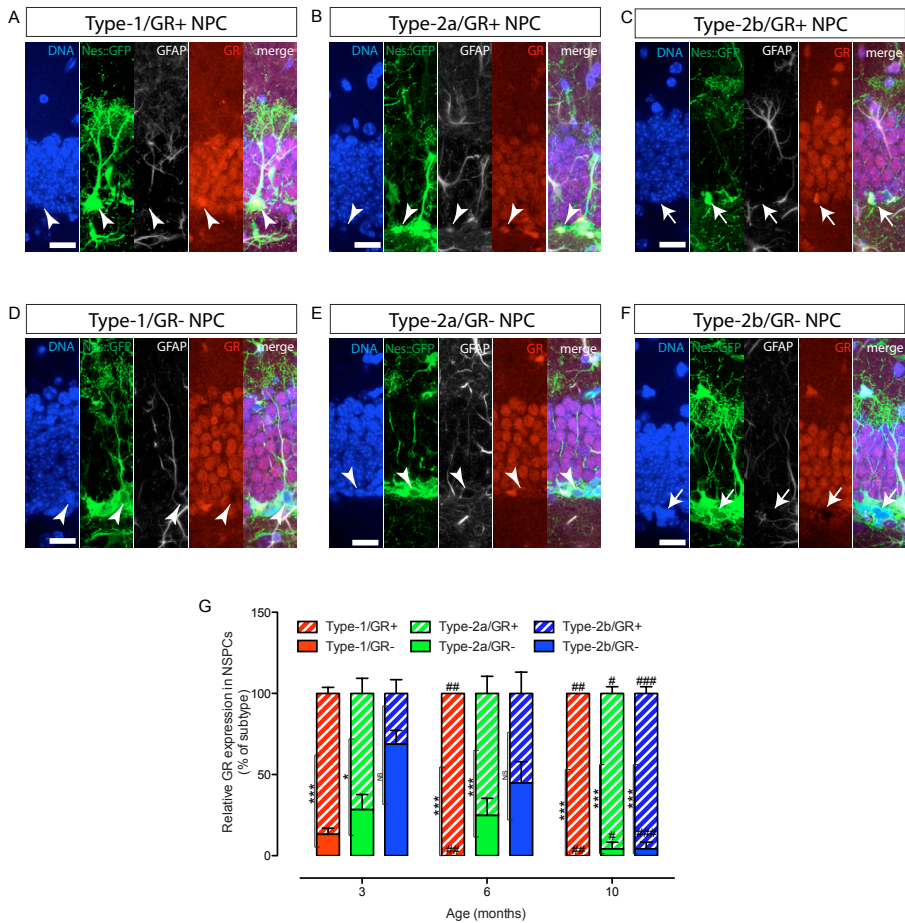


Figure 2 - Relative expression levels of GR in NPCs increases with age.

(A) Representative confocal micrograph showing an example of a Nestin-GFP+/GFAP+/GR+ NPC (arrowheads) with a characteristic vertical process and triangular cell-body in the SGZ of the DG, indicative of a type-1 NPC expressing the GR. Nuclei are visualized by a Hoechst staining (blue). (B) Representative confocal micrograph showing an example of a Nestin-GFP+/GFAP+/GR+ NPC (arrowheads) with a characteristic rounded cell-body in the SGZ of the DG, indicative of a type-2a NPC expressing the GR. Nuclei are visualized by a Hoechst staining (blue). (C) Representative confocal micrograph showing an example of a Nestin-GFP+/GFAP-/GR+ NPC (arrow) with a characteristic rounded cell-body in the SGZ of the DG, indicative of a type-2b NPC expressing the GR. Nuclei are visualized by a Hoechst staining (blue). (D) Representative confocal micrograph showing an example of a Nestin-GFP+/GFAP-/GR- NPC (arrowheads) with a characteristic vertical process and triangular cell-body in the SGZ of the DG, indicative of a type-1 NPC not expressing the GR. Nuclei are visualized by a Hoechst staining (blue). (E) Representative confocal micrograph showing an example of a Nestin-GFP+/GFAP+/GR- NPC (arrowheads) with a characteristic rounded cell-body in the SGZ of the DG, indicative of a type-2a NPC not expressing the GR. Nuclei are visualized by a Hoechst staining (blue). (F) Representative confocal micrograph showing an example of a Nestin-GFP+/GFAP-/GR- NPC (arrow) with a characteristic rounded cell-body in the SGZ of the DG, indicative of a type-2b NPC not expressing the GR. Nuclei are visualized by a Hoechst staining (blue). (G) Bar graph depicting the relative numbers of type-1/GR+ (dashed red), type-1/GR- (solid red), type-2a/GR+ (dashed green), type-2a/GR- (solid green), type-2b/GR+ (dashed blue) and type-2b/GR- (solid blue) NPC per hippocampus at 3, 6 and 10 months of age. Data are expressed as relative mean±SD of three animals and statistically tested for differences (*p < 0.05, ***p < 0.001) in GR+/GR- populations within each subtype at each time-point and for differences (#p < 0.05, ###p < 0.01, ####p < 0.001) compared to 3 months using one-way analysis of variance. Scale bars represent 20 µm (A-F).

Table 1 - Analysis of best-fit curves for Type-1/GR+ and Type-1/GR- NPC.

Type-1/GR+					Type-1/GR-				
2 nd order polynomial ($y(x) = ax^2 + bx + c$)	$y(X_{(3,10)}) = 9.3x^2 - 124.8x + 1772$				$y(X_{(3,10)}) = 16.5x^2 - 55.1x - 19.21$				
Parameters	a	b	c		a	b	c		
mean	9.3	-124.8	1778		16.5	-55.1	-19.21		
95% CI	-3.7 to 22.4	-151.2 to -98.3	1642 to 1903		3.5 to 29.6	-81.6 to -28.7	-149.4 to 110.9	to	
Goodness of fit	Degr. of freedom	R square	Abs sum squares	Sy.x	Degr. of freedom	R square	Abs sum squares	Sy.x	
	18	0.8461	463886	160.5	18	0.5482	463886	160.5	
1 st order polynomial ($y(x) = ax + b$)	$y(X_{(3,10)}) = -120.2x + 2610$				$y(X_{(3,10)}) = -46.9x + 414.0$				
Parameters	a	b			a	b			
mean	-120.2	2610			-46.9	414.0			
95% CI	-146.6 to -93.8	2426 to 2793			-76.3 to -17.6	209.7 to 618.2			
Goodness of fit	Degr. of freedom	R square	Abs sum squares	Sy.x	Degr. of freedom	R square	Abs sum squares	Sy.x	
	19	0.8270	521711	165.7	19	0.3704	646427	184.5	
Sum of squares F-test comparison of fits									
Null hypothesis	1 st order polynomial kinetics (straight line)				1 st order polynomial kinetics (straight line)				
Alternative hypothesis	2 nd order polynomial kinetics (quadratic)				2 nd order polynomial kinetics (quadratic)				
p value	0.1515				0.0159				
Conclusion ($\alpha = 0.05$)	Do not reject null hypothesis				Reject null hypothesis				
Preferred model	1 st order polynomial kinetics (straight line)				2 nd order polynomial kinetics (quadratic)				
F (DFn, DFd)	2.244 (1,18)				7.083 (1,18)				

Table 2 - Analysis of best-fit curves for Type-2a/GR+ and Type-2a/GR- NPC.

Type-2a/GR+					Type-2a/GR-				
2 nd order polynomial ($y(x) = ax^2 + bx + c$)	$y(X_{(3,10)}) = 11.9x^2 - 64.6x + 1285$				$y(X_{(3,10)}) = -3.3x^2 - 84.0x + 404.4$				
Parameters	a	b	c		a	b	c		
mean	11.9	-64.6	1285		-3.3	-84.0	404.4		
95% CI	-23.6 to 47.3	-136.4 to 7.2	932.0 to 1638		-38.7 to 32.1	-155.8 to 12.13	51.3 to 757.6	to	
Goodness of fit	Degr. of freedom	R square	Abs sum squares	Sy.x	Degr. of freedom	R square	Abs sum squares	Sy.x	
	18	0.1680	3.415e6	435.6	18	0.2713	3.415e6	435.6	
1 st order polynomial ($y(x) = ax + b$)	$y(X_{(3,10)}) = -58.8x + 1755$				$y(X_{(3,10)}) = -85.6x + 919.4$				
Parameters	a	b			a	b			
mean	-58.8	1755			-85.6	919.4			
95% CI	-127.2 to 9.7	1279 to 2230			-153.2 to -18.0	449.5 to 1389			
Goodness of fit	Degr. of freedom	R square	Abs sum squares	Sy.x	Degr. of freedom	R square	Abs sum squares	Sy.x	
	19	0.1452	3.509e6	429.7	19	0.2698	3.509e6	424.4	
Sum of squares F-test comparison of fits									
Null hypothesis	1 st order polynomial kinetics (straight line)				1 st order polynomial kinetics (straight line)				
Alternative hypothesis	2 nd order polynomial kinetics (quadratic)				2 nd order polynomial kinetics (quadratic)				
p value	0.4911				0.8479				
Conclusion ($\alpha = 0.05$)	Do not reject null hypothesis				Do not reject null hypothesis				
Preferred model	1 st order polynomial kinetics (straight line)				1 st order polynomial kinetics (straight line)				
F (DFn, DFd)	0.4942 (1,18)				0.03786 (1,18)				

Table 3 - Analysis of best-fit curves for Type-2b/GR+ and Type-2b/GR- NPC.

Type-2b/GR+					Type-2b/GR-				
2 nd order polynomial ($y(x) = ax^2 + bx + c$)	$y(X_{(3,10)}) = 3.7x^2 - 42.5x + 681.4$				$y(X_{(3,10)}) = 44.2x^2 - 282.1x + 465.1$				
Parameters	a	b	c		a	b	c		
mean	3.7	-42.5	681.4		44.2	-282.1	464.1		
95% CI	-4.9 to 12.2	-59.8 to 25.1	596.1 to 766.8		35.6 to 52.8	-299.4 to 264.7	379.7 to 550.4	to	
Goodness of fit	Degr. of freedom	R square	Abs sum squares	Sy.x	Degr. of freedom	R square	Abs sum squares	Sy.x	
	18	0.5959	199543	105.3	18	0.9849	199543	105.3	
1 st order polynomial ($y(x) = ax + b$)	$y(X_{(3,10)}) = -40.7x + 969.0$				$y(X_{(3,10)}) = -206.2x + 2476$				
Parameters	a	b			a	b			
mean	-40.7	969.0			-206.2	2476			
95% CI	-57.3 to 24.0	853.0 to 1085			-305.0 to -215.4	2165 to 2788			
Goodness of fit	Degr. of freedom	R square	Abs sum squares	Sy.x	Degr. of freedom	R square	Abs sum squares	Sy.x	
	19	0.5777	208499	104.8	19	0.8860	1.503e6	281.3	
Sum of squares F-test comparison of fits									
Null hypothesis	1 st order polynomial kinetics (straight line)				1 st order polynomial kinetics (straight line)				
Alternative hypothesis	2 nd order polynomial kinetics (quadratic)				2 nd order polynomial kinetics (quadratic)				
p value	0.3806				< 0.0001				
Conclusion ($\alpha = 0.05$)	Do not reject null hypothesis				Reject null hypothesis				
Preferred model	First order polynomial (straight line)				2 nd order polynomial kinetics (quadratic)				
F (DFn, DFd)	0.8079 (1,18)				117.6 (1,18)				

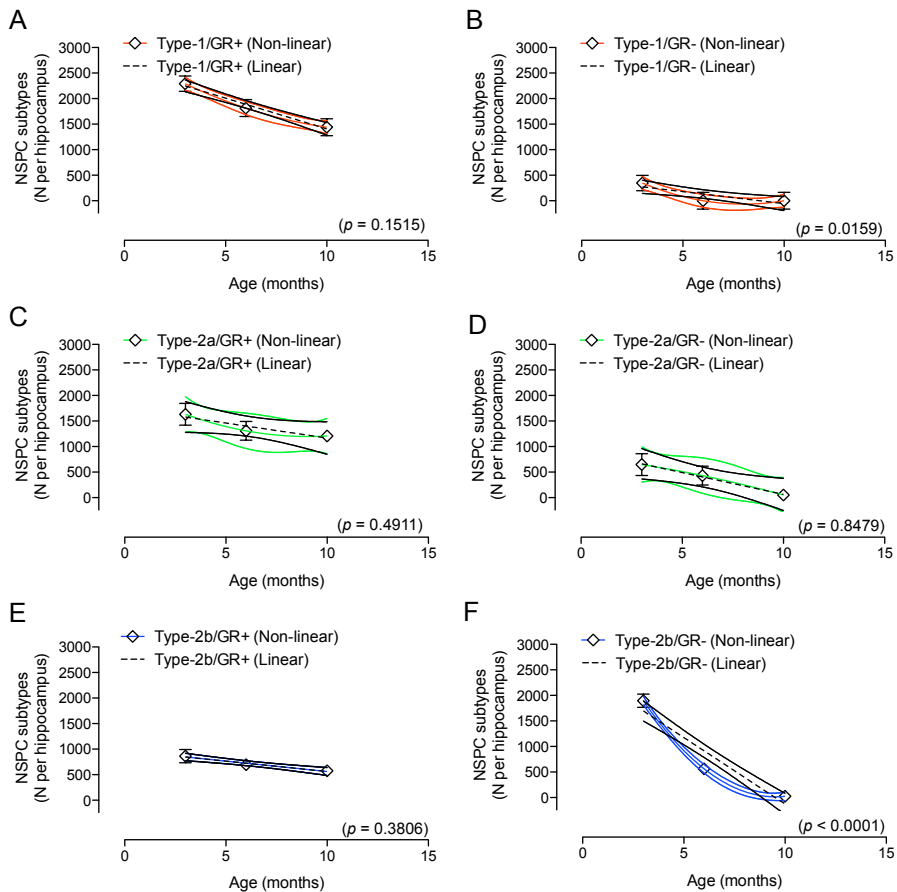


Figure 3 - Decay kinetics of Nestin-GFP expressing NPC subsets reveals differential sensitivity to age-related decline, in correlation with GR expression.

(A) Plots displaying best-fit curve comparison of age-related type-1/GR+ decay kinetics. Red line indicates a 2nd order polynomial (quadratic) curve fitting and black dotted line a 1st order polynomial (straight line) curve fitting. (B) Plots displaying best-fit curve comparison of age-related type-1/GR- decay kinetics. Red line indicates a 2nd order polynomial (quadratic) curve fitting and black dotted line a 1st order polynomial (straight line) curve fitting. (C) Plots displaying best-fit curve comparison of age-related type-2a/GR+ decay kinetics. Green line indicates a 2nd order polynomial (quadratic) curve fitting and black dotted line a 1st order polynomial (straight line) curve fitting. (D) Plots displaying best-fit curve comparison of age-related type-2a/GR- decay kinetics. Green line indicates a 2nd order polynomial (quadratic) curve fitting and black dotted line a 1st order polynomial (straight line) curve fitting. (E) Plots displaying best-fit curve comparison of age-related type-2b/GR+ decay kinetics. Blue line indicates a 2nd order polynomial (quadratic) curve fitting and black dotted line a 1st order polynomial (straight line) curve fitting. (F) Plots displaying best-fit curve comparison of age-related type-2b/GR- decay kinetics. Blue line indicates a 2nd order polynomial (quadratic) curve fitting and black dotted line a 1st order polynomial (straight line) curve fitting. Data point values (polygons) are expressed as mean \pm SEM of three animals. Best-fit curve values (lines) are expressed as mean \pm 95% confidence interval. (A-F) A 1st or 2nd order polynomial curve fitting preference using a sum of squares F-test was used within the 3-10 months domain (preferring the 2nd order model is indicated with a $p < 0.05$, p -value shown in plots).

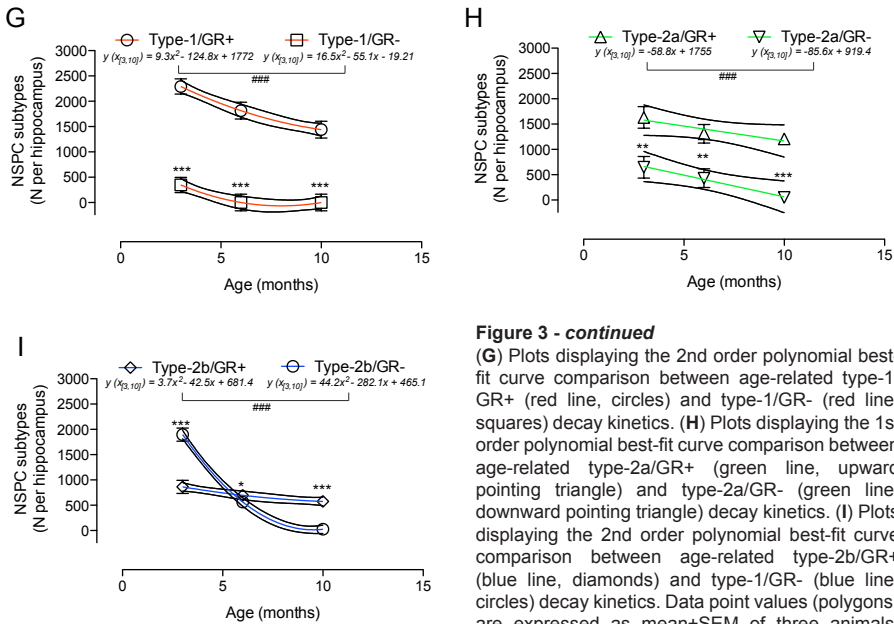


Figure 3 - continued

(G) Plots displaying the 2nd order polynomial best-fit curve comparison between age-related type-1/GR+ (red line, circles) and type-1/GR- (red line, squares) decay kinetics. (H) Plots displaying the 1st order polynomial best-fit curve comparison between age-related type-2a/GR+ (green line, upward pointing triangle) and type-2a/GR- (green line, downward pointing triangle) decay kinetics. (I) Plots displaying the 2nd order polynomial best-fit curve comparison between age-related type-2b/GR+ (blue line, diamonds) and type-1/GR- (blue line, circles) decay kinetics. Data point values (polygons) are expressed as mean±SEM of three animals. Best-fit curve values (lines) are expressed as mean±95% confidence interval. (G-I) Best-fit curves were compared for significant differences (###p < 0.001) between GR+/GR- NPC subsets using sum of squares F-test within the 3-10 months domain.

type-1/GR+ and type-2a/GR+ NPC had a significantly higher increment and smaller slope compared to type-1/GR- and type-2a/GR- NPC, respectively (Figure 3G, Table 4; Figure 3H, Table 4). Conversely, the fit curve corresponding of type-2b/GR+ NPC had a significantly lower increment and a smaller slope compared to type-2a/GR- NPC (Figure 3I, Table 4), indicating that GR expression may be associated with differences between cell population decay dynamics of type-2a and type-2b NPC in the dentate gyrus.

Discussion

The aim of this study was to characterize NPC population sensitivity to age-related decline in numbers and whether this could be coupled to GR expression levels. NPC population dynamics can be considered a multidimensional system with numbers being influenced by NPC quiescence, (asymmetric and symmetric) division, differentiation and apoptosis²⁷. Accordingly, we first analyzed which mathematical functions fitted best

to the different NPC subpopulations. Exponential functions were discarded since they did not fit well and had a very large 95% confidence interval. This uncertainty is due to a transition period between postnatal and adult neurogenesis in which NPC populations were not quantified. Quadratic and linear functions, however, fitted the data well, with good 95% confidence intervals.

Our observations confirmed that type-1 and type-2 NPCs decline selectively with age as demonstrated before^{22,25,28}, and show for the first time that this decline is associated with expression of the GR. These observations suggest that NPCs have differential age-related sensitivities to systemic factors, such as GC. Furthermore subsets of NPCs that co-express GR in the young adult hippocampus are well preserved with age, consistent with their dominance also found in middle-age mice. In addition, NPC subsets expressing the GR tended to follow age-related decay with a less drastic, linear, kinetic pattern as compared to those lacking

Table 4 - Statistical analysis of best-fit curve parameters between subsets of NPC expressing or lacking GR.

	Type-1/GR+ vs. type-1/GR- ($y(x) = ax^2 + bx + c$)	Type-2a/GR+ vs. type-2a/GR- ($y(x) = ax + b$)	Type-2b/GR+ vs. type-2b/GR- ($y(x) = ax^2 + bx + c$)
	Sum of squares <i>F</i> -test comparison of fits		
Null hypothesis	<i>a</i> , <i>b</i> and <i>c</i> same for each data set	<i>a</i> and <i>b</i> same for each data set	<i>a</i> , <i>b</i> and <i>c</i> same for each data set
Alternative hypothesis	<i>a</i> , <i>b</i> and <i>c</i> different for each data set	<i>a</i> and <i>b</i> different for each data set	<i>a</i> , <i>b</i> and <i>c</i> different for each data set
<i>p</i> value	< 0.0001	< 0.0001	< 0.0001
Conclusion ($\alpha = 0.05$)	Reject null hypothesis	Reject null hypothesis	Reject null hypothesis
Preferred model	<i>a</i> , <i>b</i> and <i>c</i> different for each data set	<i>a</i> and <i>b</i> different for each data set	<i>a</i> , <i>b</i> and <i>c</i> different for each data set
F (DFn, DFd)	413.7 (3, 36)	29.25 (2,38)	145.9 (3, 36)

GR expression, suggesting the GR may be involved in controlling age-related decay.

The age-related loss or deforestation of NPC has been proposed as a critical factor contributing to a decline in AHN with age²⁹. The Nestin-GFP mice used in these study represent a suitable model to study this decay. Importantly, potential difference in half-life time of Nestin versus GFP may not confound the interpretation of the relative abundance of GFP+/GFAP+ NPC populations in these transgenic mice¹⁸. Accordingly, in contrast to previous interpretations of GR expression patterns in NPC²¹ from our results it could be speculated that the GR is involved controlling age-related NPC decay under basal conditions. Consistent with this, retroviral-mediated knock-down of the GR in NPCs *in vivo*, resulted in increased neurogenesis and accelerated NPC differentiation under basal stress-free conditions¹⁹. Therefore, our current and previous results combined suggest that GR expression may prevent NPC to prematurely undergo differentiation and thus indirectly favor an undifferentiated, proliferative phenotype. However, the specific mechanisms involved remain uncharacterized and are beyond the aim of this study. In agreement with our interpretation, lowering the enhanced CORT levels observed at old age (20-26 month-old rats) may release NPC from a CORT-induced quiescent state³⁰. However, contrasting observations have been made when CORT levels were lowered from postnatal day 10 onwards³¹, emphasizing the age-dependent role of GC in the regulation of NPC.

It has been suggested that some aspects of the aging process are influenced by systemically secreted factors, which may inhibit AHN, including GC³⁰. Attributed to a decreased amplitude but not maximum concentrations, basal daily rhythmicity of CORT secretion is one of the factors that has

been described to flatten with age^{6,7}, with a concomitant AHN decrease¹¹. Although this 'flattened CORT release' phenotype cannot be further aggravated by e.g. increasing CORT levels³², adrenalectomy can restore the age dependent decrease in AHN³⁰. A possible interpretation of this seemingly contradictory data can be two-fold, i.e. on the one hand, lowering CORT levels per se appears sufficient to enhance AHN, on the other, a loss of the pulsatile nature of basal CORT release could be involved in the regulation of AHN as well, providing a distinct signal controlling NPC proliferation (**chapter 5**).

While a number of previous studies have described general decreases in AHN with age¹², a recent study has analyzed in more detail the age-related reduction of type-1 and type-2 NPCs specifically²². This was also based on the expression of Nestin-GFP and their respective radial or horizontal morphologies as in our current study. Interestingly, these authors found type-1 NPCs to gradually decrease whereas type-2 NPCs showed a more dramatic reduction between 6 and 9 months²², in agreement with our observations.

Additionally, other studies quantified age-related reductions in NPCs based on Notch signaling activity. Using Hes5::GFP reporter mice, Lugert *et al.* could identify both horizontal and radial NPC populations and found the levels of the former to decrease with increasing age and the levels of the latter to remain stable²⁵. These differences regarding the age-dependent reduction in both subpopulations of NPCs, as compared with our observations, may arise from experimental differences including different antibodies used for the detection of cell-specific markers. Importantly, Lugert *et al.* examined NPC levels at different ages in heterogeneous groups of animals in

terms of age and sex of the animals, which is an important factor affecting AHN⁹ was not discriminated in this study²⁵. Furthermore, it is unclear to what extent Hes5::GFP and Nestin-GFP expression overlap in the adult hippocampus, and thus whether they would identify exactly the same NPC populations. Interestingly, it has previously been demonstrated that Notch activity, as measured through Hes5 expression, promotes NPC self-renewal provided it follows an oscillatory nature, whereas sustained Notch activity induces differentiation³³, indicating that quiescent NPCs, actively proliferating NPCs and differentiating newborn cells can all be Hes5+ or Hes5-³⁴.

In theory, a decline in AHN can be achieved through changes in quiescence, proliferation, apoptosis and differentiation of type-1 and type-2 NPC subtypes. Our data show that GR- and GR+ type-2 NPC subsets harbor different age-related decay kinetics, with GR-/type-2a NPC preferentially following linear decay kinetics, while GR+/type-2b NPC followed non-linear decay kinetics. Interestingly, previous reports have described a differential apoptotic sensitivity between the type-1, 2a and 2b NPC, with the latter displaying the highest sensitivity to apoptosis³⁵, possibly contributing to the non-linear decay kinetics of type-2b/GR- NPC. Suggestively, we have previously described a link between active caspase-3 mediated NPC apoptosis and differentiation, that could be directed by GR activation¹⁹. Accordingly, it is possible that type-2b cell numbers are influenced by their relative levels of proliferation, apoptosis and differentiation, all of which can be regulated by the GR. This could explain the dramatic age-related decrease of type-2b/GR- NPC compared to type-2b/GR+ NPC.

Our observations are generally comparable to those made earlier by Garcia *et al.* regarding the relative increases in NPCs (co-)expressing the GR with age²¹. In contrast though, we detected higher levels of type-1/GR+ NPCs at young age and found GR immunoreactivity in type-2b NPC, which could be due to differences in primary GR antibodies and in the Nestin-GFP transgenic strain used. Another likely scenario could be the sex differences between our study and those described by Garcia *et al.*²¹ since e.g. sex hormones could underly gender

specific expression of the GR in NPC. Indeed, a considerable body of evidence has highlighted the cross-talk between glucocorticoids and sex hormones through their respective receptors³⁶⁻³⁸ while previous reports describe both an age dependent increase in CORT levels yet a decrease in both male and female sex hormones³⁻⁵.

In conclusion, a role for the GR in disfavoring a proliferative phenotype in NPC with age could explain previous observations concerning differences in the relative age-related stability of NPC subsets. This suggests a GR-mediated protective effect on NPC decay or 'deforestation'²⁹ and/or quiescence/senescence^{22,25,39}. Further analysis should address important questions arising from this hypothesis, such as to which extent this protective effect is mediated by alterations in symmetric vs. asymmetric NPC self-renewal, apoptosis or persistent quiescence.

Together, our data suggest that age-associated changes in HPA axis activity could contribute to the differential maintenance or decline of specific hippocampal NPC populations and thus to their neurogenic potential into older age.

References

1. Lightman, S. L. & Conway-Campbell, B. L. The crucial role of pulsatile activity of the HPA axis for continuous dynamic equilibration. *Nat. Rev. Neurosci.* 11, 710–718 (2010).
2. Lucassen, P. J. et al. Regulation of adult neurogenesis by stress, sleep disruption, exercise and inflammation: Implications for depression and antidepressant action. *Eur Neuropsychopharmacol* 20, 1–17 (2010).
3. Guazzo, E. P., Kirkpatrick, P. J., Goodyer, I. M., Shiers, H. M. & Herbert, J. Cortisol, dehydroepiandrosterone (DHEA), and DHEA sulfate in the cerebrospinal fluid of man: relation to blood levels and the effects of age. *J. Clin. Endocrinol. Metab.* 81, 3951–3960 (1996).
4. McEwen, B., de Leon MJ, Lupien, S. & Meaney, M. Corticosteroids, the Aging Brain and Cognition. *Trends Endocrinol. Metab.* 10, 92–96 (1999).
5. Kalmijn, S. et al. A prospective study on cortisol, dehydroepiandrosterone sulfate, and cognitive function in the elderly. *J. Clin. Endocrinol. Metab.* 83, 3487–3492 (1998).
6. Van Cauter, E., Leproult, R. & Plat, L. Age-related changes in slow wave sleep and REM sleep and relationship with growth hormone and cortisol levels in healthy men. *JAMA* 284, 861–868 (2000).

7. van Coevorden, A. et al. Neuroendocrine rhythms and sleep in aging men. *Am. J. Physiol.* 260, E651–61 (1991).
8. Wang, Q. et al. Glucocorticoid receptor protein expression in human hippocampus; stability with age. *Neurobiol. Aging* 34, 1662–1673 (2013).
9. Naninck, E. F. G. et al. Chronic early life stress alters developmental and adult neurogenesis and impairs cognitive function in mice. *Hippocampus* 25, 309–328 (2015).
10. Snyder, J. S., Soumier, A., Brewer, M., Pickel, J. & Cameron, H. A. Adult hippocampal neurogenesis buffers stress responses and depressive behaviour. *Nature* 476, 458–461 (2011).
11. Seib, D. R. M. & Martin-Villalba, A. Neurogenesis in the Normal Ageing Hippocampus: A Mini-Review. *Gerontology* 61, 327–335 (2015).
12. Kuhn, H. G., Dickinson-Anson, H. & Gage, F. H. Neurogenesis in the dentate gyrus of the adult rat: age-related decrease of neuronal progenitor proliferation. *J. Neurosci.* 16, 2027–2033 (1996).
13. Seri, B., Garcia-Verdugo, J. M., McEwen, B. S. & Alvarez-Buylla, A. Astrocytes give rise to new neurons in the adult mammalian hippocampus. *J. Neurosci.* 21, 7153–7160 (2001).
14. Seri, B., García-Verdugo, J. M., Collado-Morente, L., McEwen, B. S. & Alvarez-Buylla, A. Cell types, lineage, and architecture of the germinal zone in the adult dentate gyrus. *J. Comp. Neurol.* 478, 359–378 (2004).
15. Ming, G.-L. & Song, H. Adult neurogenesis in the mammalian central nervous system. *Annu. Rev. Neurosci.* 28, 223–250 (2005).
16. Kempermann, G., Jessberger, S., Steiner, B. & Kronenberg, G. Milestones of neuronal development in the adult hippocampus. *Trends Neurosci.* 27, 447–452 (2004).
17. Steiner, B. et al. Type-2 cells as link between glial and neuronal lineage in adult hippocampal neurogenesis. *Glia* 54, 805–814 (2006).
18. Mignone, J. L., Kukekov, V., Chiang, A.-S., Steindler, D. & Enikolopov, G. Neural stem and progenitor cells in nestin-GFP transgenic mice. *J. Comp. Neurol.* 469, 311–324 (2004).
19. Fitzsimons, C. P. et al. Knockdown of the glucocorticoid receptor alters functional integration of newborn neurons in the adult hippocampus and impairs fear-motivated behavior. *Mol. Psychiatry* 18, 993–1005 (2013).
20. Cameron, H. A., Woolley, C. S. & Gould, E. Adrenal steroid receptor immunoreactivity in cells born in the adult rat dentate gyrus. *Brain Res.* 611, 342–346 (1993).
21. Garcia, A., Steiner, B., Kronenberg, G., Bick-Sander, A. & Kempermann, G. Age-dependent expression of glucocorticoid- and mineralocorticoid receptors on neural precursor cell populations in the adult murine hippocampus. *Aging Cell* 3, 363–371 (2004).
22. Romine, J., Gao, X., Xu, X.-M., So, K. F. & Chen, J. The proliferation of amplifying neural progenitor cells is impaired in the aging brain and restored by the mTOR pathway activation. *Neurobiol. Aging* 36, 1716–1726 (2015).
23. Flurkey, K., Curren, J. M. & Harrison, D. E. 'Mouse models in aging research.' by K Flurkey, J M Curren et al. (2007).
24. van Hooijdonk, L. W. A. et al. Lentivirus-mediated transgene delivery to the hippocampus reveals sub-field specific differences in expression. *BMC Neurosci* 10, 2 (2009).
25. Lugert, S. et al. Quiescent and active hippocampal neural stem cells with distinct morphologies respond selectively to physiological and pathological stimuli and aging. *Cell Stem Cell* 6, 445–456 (2010).
26. Fitzsimons, C. P. et al. The microtubule-associated protein doublecortin-like regulates the transport of the glucocorticoid receptor in neuronal progenitor cells. *Mol. Endocrinol.* 22, 248–262 (2008).
27. Ziebell, F., Martin-Villalba, A. & Marciniak-Czochra, A. Mathematical modelling of adult hippocampal neurogenesis: effects of altered stem cell dynamics on cell counts and bromodeoxyuridine-labelled cells. *J R Soc Interface* 11, 20140144–20140144 (2014).
28. Spalding, K. L. et al. Dynamics of hippocampal neurogenesis in adult humans. *Cell* 153, 1219–1227 (2013).
29. Encinas, J. M. & Sierra, A. Neural stem cell deforestation as the main force driving the age-related decline in adult hippocampal neurogenesis. *Behav. Brain Res.* 227, 433–439 (2012).
30. Cameron, H. A. & McKay, R. D. Restoring production of hippocampal neurons in old age. *Nat. Neurosci.* 2, 894–897 (1999).
31. Brunson, K. L., Baram, T. Z. & Bender, R. A. Hippocampal neurogenesis is not enhanced by lifelong reduction of glucocorticoid levels. *Hippocampus* 15, 491–501 (2005).
32. Heine, V. M., Maslam, S., Joels, M. & Lucassen, P. J. Prominent decline of newborn cell proliferation, differentiation, and apoptosis in the aging dentate gyrus, in absence of an age-related hypothalamus-pituitary-adrenal axis activation. *Neurobiol. Aging* 25, 361–375 (2004).
33. Imayoshi, I. et al. Oscillatory control of factors determining multipotency and fate in mouse neural progenitors. *Science* 342, 1203–1208 (2013).
34. Giachino, C. & Taylor, V. Notching up neural stem cell homogeneity in homeostasis and disease. *Front Neurosci* 8, 32 (2014).
35. Sierra, A. et al. Microglia shape adult hippocampal neurogenesis through apoptosis-coupled phagocytosis. *Cell Stem Cell* 7, 483–495 (2010).
36. Cvorc, A. et al. Cross talk between glucocorticoid and estrogen receptors occurs at a subset of proinflammatory genes. *J. Immunol.* 186, 4354–4360 (2011).

37. Karmakar, S., Jin, Y. & Nagaich, A. K. Interaction of glucocorticoid receptor (GR) with estrogen receptor (ER) α and activator protein 1 (AP1) in dexamethasone-mediated interference of ER α activity. *J. Biol. Chem.* 288, 24020–24034 (2013).
38. Zhang, Y., Leung, D. Y. M., Nordeen, S. K. & Goleva, E. Estrogen inhibits glucocorticoid action via protein phosphatase 5 (PP5)-mediated glucocorticoid receptor dephosphorylation. *J. Biol. Chem.* 284, 24542–24552 (2009).
39. Lazarov, O., Mattson, M. P., Peterson, D. A., Pimplikar, S. W. & van Praag, H. When neurogenesis encounters aging and disease. *Trends Neurosci.* 33, 569–579 (2010).